CMLS, Cell. Mol. Life Sci. 61 (2004) 669–681
1420-682X/04/060669-13
DOI 10.1007/s00018-003-3316-0

CMLS Cellular and Molecular Life Sciences

Review

Glutamate synthase: a fascinating pathway from L-glutamine to L-glutamate

R. H. H. van den Heuvel[a, b], B. Curti[c], M. A. Vanoni[c, *] and A. Mattevi[a, *]

[a] Department of Genetics and Microbiology, University of Pavia, via Abbiategrasso 207, 27100 Pavia (Italy), e-mail: mattevi@ipvgen.unipv.it
[b] Department of Biomolecular Mass Spectrometry, Bijvoet Center for Biomolecular Research and Utrecht Institute for Pharmaceutical Sciences, Utrecht University, Sorbonnelaan 16, 3584 CA Utrecht (The Netherlands)
[c] Department of Biomolecular Sciences and Biotechnology, University of Milan, via Celoria 26, 20133 Milan (Italy), e-mail: Maria.Vanoni@unimi.it

Received 8 August 2003; received after revision 15 September 2003; accepted 17 September 2003

Abstract. Glutamate synthase is a multicomponent iron-sulfur flavoprotein belonging to the class of N-terminal nucleophile amidotransferases. It catalyzes the conversion of L-glutamine and 2-oxoglutarate into two molecules of L-glutamate. In recent years the X-ray structures of the ferredoxin-dependent glutamate synthase and of the α subunit of the NADPH-dependent glutamate synthase have become available. Thanks to X-ray crystallography, it is now known that the ammonia reaction intermediate is transferred via an intramolecular tunnel from the amidotransferase domain to the synthase domain over a distance of about 32 Å. Although ammonia channeling is a recurrent theme for N-terminal nucleophile and triad-type amidotransferases, the molecular mechanisms of ammonia transfer and its control are different for each known amidotransferase. This review focuses on the intriguing mechanism of action and self-regulation of glutamate synthase with a special focus on the structural data.

Key words. Glutamine-dependent amidotransferase; glutamate synthase; substrate channeling; crystal structure; multicomponent enzyme; ammonia tunnel; electrospray ionization mass spectrometry.

Introduction

In this review we address the fascinating mechanism of action of the multicomponent glutamine-dependent amidotransferase glutamate synthase, hereafter referred to as GltS, with a special focus on recent structural data. The review on GltS of Vanoni and Curti in 1999 [1] in this journal provides the necessary background information on the enzyme and is an excellent introduction for this review.
Recent X-ray crystallographic data have revealed that the iron-sulfur and flavin-dependent GltS functions through the intramolecular transfer of ammonia between functionally distinct domains (namely amidotransferase and flavin mononucleotide (FMN) binding domains) over a distance of about 32 Å [2–4]. Moreover, GltS is only active when both L-glutamine and 2-oxoglutarate substrates are bound, the enzyme is in the reduced state and, in the case of ferredoxin-dependent GltS, in complex with reduced ferredoxin, hereafter referred to as Fd [5, 6]. Thus, GltS has evolved a sophisticated mechanism to control and coordinate catalytic activities at sites physically distinct from each other, and to channel the reaction intermediate between catalytic sites.

Biochemistry of glutamate synthase

Prior to 1970 it was generally assumed that ammonia was assimilated by direct assimilation of 2-oxoglutarate to

* Corresponding authors.

produce L-glutamate in a single NAD(P)H-linked reaction catalyzed by the enzyme glutamate dehydrogenase. The pioneering work of Tempest and co-workers [7] demonstrated the existence of a glutamine synthetase/glutamate synthase pathway, which is operative in bacteria growing on media with a low ammonia content, or in bacteria devoid of glutamate dehydrogenases or equivalent amino acid dehydrogenases. Further studies revealed that the concerted action of glutamine synthetase and GltS is responsible for primary and secondary ammonia assimilation also in plants (as reviewed in [8] and [9]). The glutamine synthetase (GS)/glutamate synthase pathway, also known as the GS/GOGAT pathway from the now obsolete acronym for GltS, is of crucial importance in microbial and plant cells, as the products L-glutamine and L-glutamate are the nitrogen donors for the biosynthesis of major nitrogen-containing compounds, including, for example, other amino acids, nucleotides, chlorophylls, polyamines and alkaloids [10, 11]. GltS is a ubiquitous enzyme in nature; it has been detected in prokaryotes, archaea and eukaryotes. However the enzyme has not been found in higher eukaryotic systems such as *Homo sapiens*. The enzyme catalyzes the reductant-dependent conversion of 2-oxoglutarate into L-glutamate in which L-glutamine serves as the nitrogen source for the reaction. The overall catalytic cycle of GltS can be described by the following equation in which the reducing equivalents originate from NADH, NADPH or reduced Fd, depending on the type of GltS:

$$\text{L-glutamine} + \text{2-oxoglutarate} + 2e^- \rightarrow 2\ \text{L-glutamate} \quad (1)$$

The catalytic cycle (equation 1) involves distinct catalytic reactions (fig. 1). After enzyme reduction, L-glutamine is hydrolyzed to yield ammonia and L-glutamate via a glutamyl thioester-cysteine intermediate. This reaction is followed by the addition of ammonia onto 2-oxoglutarate, forming 2-iminoglutarate. 2-Iminoglutarate is then subject to reduction by a reduced flavin cofactor, forming the second molecule of L-glutamate.

On the basis of the primary structures of GltSs from different sources and the known biochemical properties, three distinct classes of GltS can be distinguished [1]:

1) Ferredoxin-dependent GltS (Fd-GltS) is an iron-sulfur and FMN-containing enzyme that has been detected in chloroplasts of higher plants, cyanobacteria and algae. This enzyme is composed of a single polypeptide chain with a molecular mass of about 165 kDa. The enzyme functions through the noncovalent binding of a reduced

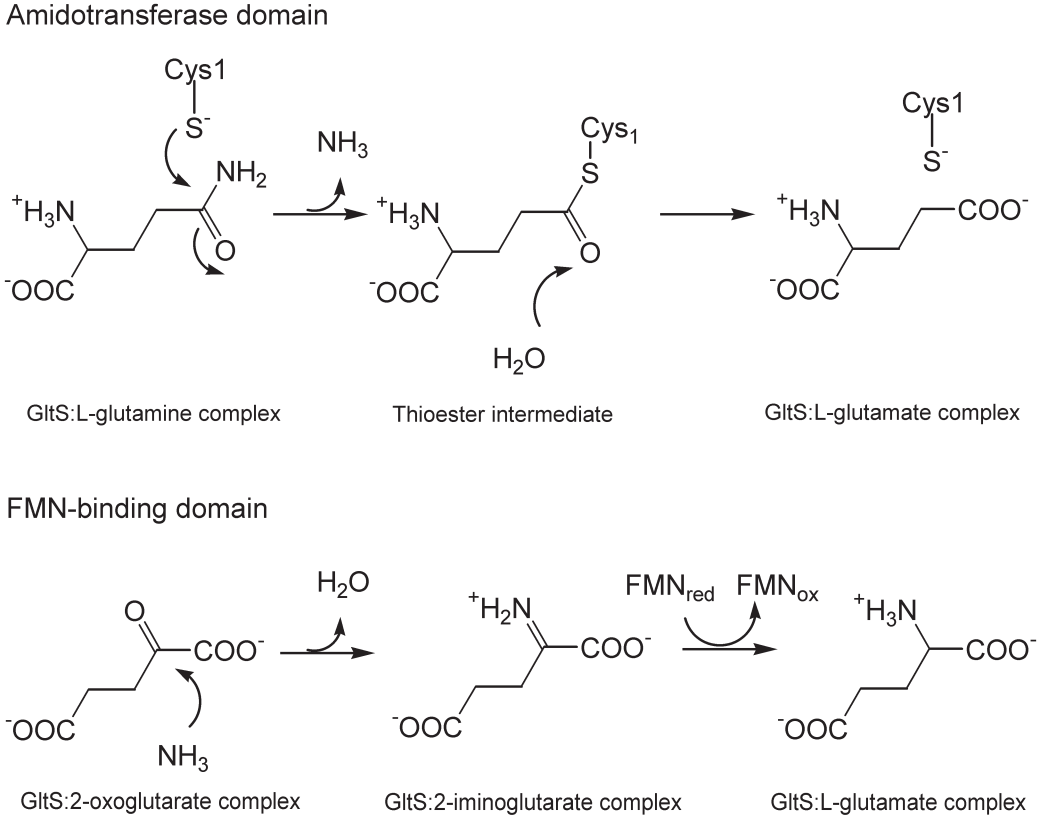

Figure 1. Schematic representation of the partial reactions catalyzed by GltS leading to glutamine-dependent glutamate synthesis. The ammonia produced in the amidotransferase domain is added onto 2-oxoglutarate in the FMN binding domain. The reducing equivalents originate from reduced ferredoxin (Fd-GltS) or NADPH (through the NADPH β-GltS subunit and the corresponding part of NADH-GltS). Note that the precise protonation states of intermediates and active site residues are unknown.

Fd molecule, which delivers the reducing equivalents via the $[3Fe\text{-}4S]^{0,+1}$ cluster to the FMN prosthetic group. Biochemical data are available from spinach and *Synechocystis* sp. Fd-GltS [5, 12, 13], whereas the X-ray structure is known for the *Synechocystis* enzyme [3, 4].

2) The NADPH-dependent GltS (NADPH-GltS) is mostly found in bacteria. The enzyme is composed of two tightly bound dissimilar subunits, which form the $\alpha\beta$ holoenzyme containing one flavin adenine dinucleotide (FAD) and one FMN cofactor, and three distinct iron-sulfur clusters: one $[3Fe\text{-}4S]^{0,+1}$ center and two low potential $[4Fe\text{-}4S]^{+1,+2}$ clusters. The larger (α) subunit (160 kDa) catalyzes the reductive synthesis of L-glutamate from L-glutamine and 2-oxoglutarate [14]. The smaller (β) subunit (52 kDa) is a FAD-dependent NADPH oxidoreductase [15]. It serves to transfer reducing equivalents from NADPH to the FMN cofactor (on the α subunit) through the FAD cofactor (on the β subunit) and at least two of the NADPH-GltS three iron-sulfur clusters, namely: the $[3Fe\text{-}4S]^{0,+1}$ and one of the two low potential $[4Fe\text{-}4S]^{+1,+2}$ centers of the enzyme. Most of the information on this class of enzymes derives from work done in our laboratories on the *Azospirillum brasilense* enzyme. The three-dimensional structure of the α subunit of this enzyme has been solved [2].
3) NADH-dependent GltS is poorly characterized and is mainly found in fungi, lower animals and nongreen tissues like seeds and roots of plants. The enzyme is composed of a single polypeptide chain of about 200 kDa. Sequence analyses suggest that the enzyme is derived from a fusion of the genes coding for the α and β subunits of the NADPH-dependent enzyme. Unlike NADPH-GltS, the eukaryotic pyridine nucleotide-dependent form of GltS is highly specific for NADH as the electron donor.

GltS is a member of the glutamine-dependent amidotransferase family of enzymes. These enzymes catalyze the transfer of the amide group of L-glutamine, the source of nitrogen for most biosynthetic pathways, to an acceptor substrate, which is different for each glutamine-dependent amidotransferase, to produce one molecule of L-glutamate and one molecule of aminated (or amidated) product. To date 13 different glutamine-dependent amidotransferases have been identified [16–19]. The enzymes are involved in the biosynthesis of nucleotides, amino acids, aminated sugars and antibiotics. All amidotransferases exhibit a modular organization with physically distinct catalytic centers for L-glutamine hydrolysis and the addition of ammonia to the acceptor substrate, respectively, which are connected by an intramolecular ammonia tunnel. The amidotransferase family can be divided in four different classes: the N-terminal nucleophile (Ntn), the triad, the amidase and the nitrilase class [17, 20, 21]. The amidase and nitrilase family are only poorly characterized. Functionally, the main differences between the Ntn and triad type are the location of the catalytic cysteine residue and the mechanisms of activation of the cysteinyl thiol. In the triad amidotransferases the catalytic cysteine is found to be part of the catalytic triad Cys-His-Glu in which the His and Glu residues are postulated to activate the cysteine thiol group. In the Ntn-type amidotransferases the catalytic cysteine is located at the N-terminus of the mature protein, and activation of the cysteinyl thiol is assisted by the free amino-terminal group [19]. Furthermore, no similarity between amidotransferases of the different classes is found at the primary and tertiary structure level. Finally, as we shall discuss later, both the intramolecular tunnel for ammonia transfer and the synthase function are unrelated to each other in different amidotransferases even within each one of the four known classes of enzymes. GltSs are unique among Ntn-type amidotransferases in that they catalyze an oxidoreduction reaction, which appears to contribute a further layer of both complexity and control over the catalytic activity of the enzymes.

The glutamate synthase structure

In this review we focus on Fd-GltS from *Synechocystis* sp. and NADPH-GltS from *A. brasilense* as the two best-studied GltSs. Fd-GltS and the α subunit of NADPH-GltS are rather similar enzymes of about 160–165 kDa as also indicated by the high amino acid sequence identity (45%). Crystal structures of *A. brasilense* GltS α subunit and of several forms of Fd-GltS from *Synechocystis* sp. are available (table 1). Here, we shall mainly focus on the Fd-GltS structures since they have been solved at higher resolution.

The tertiary structures of the α subunit of NADPH-GltS and Fd-GltS, as determined by X-ray crystallography, are similar as also indicated by the root mean square deviation of 1.7 Å for all topological equivalent Cα atoms. Each GltS monomer can be described in terms of four distinct domains with different function and topology (fig. 2). Doolittle and co-workers screened 16 strains from *Thermotoga* and other related *Thermotogales* for the occurrence of the archaeal α subunit of GltS. The results clearly showed that the different domains in GltS are indeed recruited from preexisting domains [22]. The N-terminal amidotransferase domain (residues 1–422 according to Fd-GltS numbering, which will be used throughout unless otherwise stated) is characterized by a classical four-layer $\alpha/\beta/\beta/\alpha$ topology similar to that of the three other characterized Ntn-type amidotransferases. Indeed, superpositions of Fd-GltS onto glutamine phosphoribosylpyrophosphate amidotransferase (root mean square deviation 2.5 Å for 217 Cα atoms) [23], glucosamine 6-phosphate synthase (root mean square deviation 2.9 Å for

Table 1. Known X-ray structures of glutamate synthase.

Enzyme	Resolution (Å)	Ligands amidotransferase domain	Ligands FMN-binding domain	PDB entry	Reference
α-GltS[a]	3.0	L-methionine sulphone	2-oxoglutarate	1EA0	[2]
Fd-GltS[b]	2.7	–	2-oxoglutarate	1LLW	[3]
Fd-GltS[b,c]	3.0	–	–	1LLZ	[3]
Fd-GltS[b]	2.8	–	–	1LM1	[3]
Fd-GltS[b]	2.0	–	2-oxoglutarate	1OFD	[4]
Fd-GltS[b]	2.45	5-oxo-L-norleucine	–	1OFE	[4]

[a] GltS from *A. brasilense.*
[b] GltS from *Synechocystis* sp.
[c] The FMN cofactor in the GltS crystallographic model is in the reduced state.

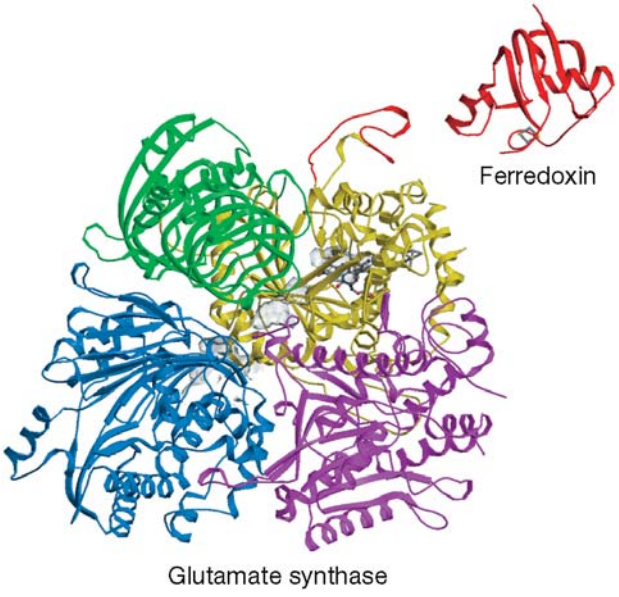

Figure 2. Tertiary structures of the Fd-GltS and Fd monomers. The N-terminal amidotransferase domain is depicted in cornflower blue, the FMN-binding domain in yellow, the central domain in magenta and the C-terminal domain in green. The Fd molecule is depicted in red. The FMN cofactor and the iron-sulfur clusters are shown as ball-and-stick, the Fd-binding loop in red and the cavities in grey. The position of Fd relative to Fd-GltS is not based on experimental evidence. The surface of active site cavities and the internal ammonia tunnel are shown. This drawing was prepared with CONSCRIPT [47] and Raster3D [48].

217 Cα atoms) [24] and asparagine synthetase B (root mean square deviation 5.2 Å for 185 Cα atoms) [25] reveal close structural similarity.

The FMN binding domain consists of residues 787–1223 and forms, next to the amidotransferase domain, the second catalytic domain in GltS. This domain has a typical $(\beta/\alpha)_8$ barrel topology and contains the $[3Fe\text{-}4S]^{0,+1}$ cluster and the FMN prosthetic group of the enzyme. The $(\beta/\alpha)_8$ barrel of the GltS FMN binding domain resembles that of other FMN binding enzymes. The most similar structures as found by DALI [26] are the FMN binding domains of flavocytochrome b_2 (root mean square deviation 3.1 Å for 254 Cα atoms) [27], glycolate oxidase (root mean square deviation 3.2 Å for 278 Cα atoms) [28] and dihydroorotate dehydrogenase (root mean square deviation 3.2 Å for 221 Cα atoms) [29]. The highest level of structural similarity is found in the core of this domain, which is the FMN binding region. A BLAST homology search revealed a unique peptide stretch in Fd-GltS, absent in NADPH-GltS α subunit and the corresponding part of NADH-GltS. These 26 residues (residues 907–933), located on the surface of the protein in the vicinity of the [3Fe-4S] cluster and the FMN cofactor, are highly conserved in all Fd-GltSs. We have proposed that reduced Fd can bind near this peptide stretch (hereafter referred to as the Fd-binding loop) to transfer an electron via the [3Fe-4S] cluster to the FMN for 2-iminoglutarate reduction [3]. To our best knowledge, Fd-GltS is the only Fd-dependent enzyme in which such a potential Fd-binding loop is recognized.

Like the FMN binding domain, the central domain (residues 423–786) is characterized by an β/α topology. Binda and co-workers [2] have demonstrated that this domain is an extended half $(\beta/\alpha)_8$ barrel as its core consists of five consecutive β/α units that generate a parallel β sheet flanked on one side by four α helices and on the other side by a single α helix running perpendicular to the sheet axis. Remarkably, DALI [26] revealed high structural similarity with the FMN-binding enzymes glycolate oxidase and dihydroorotate dehydrogenase (root mean square deviations 2.6 Å for 189 Cα atoms and 3.7 Å for 179 Cα atoms, respectively). In addition, in spite of the low sequence identity with the GltS FMN binding domain, the central and FMN binding domains are structurally similar [2]. Structural similarity was also identified with the HisF protein fragment of imidazole glycerol phosphate synthase (root mean square deviation 3.2 Å for 123 Cα atoms) [30]. HisF consists of a $(\beta/\alpha)_8$ barrel with a twofold repeat pattern. It is postulated and verified by protein engineering that HisF has evolved by a twofold gene duplication and gene fusion from a common half-barrel ancestor [30, 31]. A fascinating question is whether also the extended half $(\beta/\alpha)_8$ barrel of the GltS central domain derives from an ancient half $(\beta/\alpha)_8$ barrel.

The C-terminal GltS residues 1224–1523 form a right-handed β helix that comprises seven helical turns. The cross-section of the β helix has an ellipsoidal shape, and the helix axis extends for 43 Å. A DALI [26] search revealed that the structural similarity of this domain with other β helices is only remote. The highest structural similarity was found with polygalacturonase from *Erwinia carotovora* [32] and pectate lyase from *Bacillus* sp. [33] (root mean square deviation of 4.1 Å for 150 residues and 3.2 Å for 126 residues, respectively). In contrast to the C-terminal domain in GltS, these β helices in polygalacturonases perform a catalytic reaction, namely the hydrolysis of the α-1,4-glycosidic bond in polygalacturonic acids. The role of the C-terminal β helix in GltS is unknown. However, recent modeling studies, based on synchrotron radiation X-ray scattering measurements on solutions of NADPH-GltS α subunit, indicate that in this enzyme the C-terminal β helix may contribute to tetramerization of α subunits by interacting with the glutamine amidotransferase domain of the adjacent one [34].

Quaternary structure of glutamate synthase

Small-angle X-ray scattering data have provided evidence that Fd-GltS is a monomeric protein in solution [4]. In contrast, nanoflow electrospray ionization mass spectrometry experiments of Fd-GltS revealed that the protein is in equilibrium between the monomeric and dimeric form with m/z values around 7000 and 9000, respectively (fig. 3) [A. J. R. Heck and R. H. H. van den Heuvel, unpublished]. The molecular mass of Fd-GltS monomer determined by mass spectrometry is 166,222 Da, which is in close agreement with the mass calculated on the basis of the amino acid sequence of the mature holoprotein (166,230 Da) considering the noncovalently bound FMN cofactor (457 Da) and the [3Fe-4S] cluster (296 Da). The X-ray data of Fd-GltS have shown that the enzyme is dimeric in the crystalline state [3, 4]. We have to take into account, however, that the results obtained by any of the three techniques cannot be directly related to each other, although several reports have revealed that no major differences are to be expected at least when working at the same protein concentration, pH and ionic strength. Discrepancies in the oligomerization state were also found for the α subunit of NADPH-GltS. Small-angle X-ray scattering experiments indicated tetrameric assemblies of the α subunit of NADPH-GltS [34], whereas X-ray analysis of the crystalline protein clearly reveals dimers [2]. On the contrary, a good match between the oligomerization state of NADPH-GltS $\alpha\beta$ holoenzyme determined by small-angle X-ray scattering [34] and analytical gel filtration [36] has been observed. Indeed, both techniques indicate that the enzyme forms tetramers at concentrations above 5 µM.

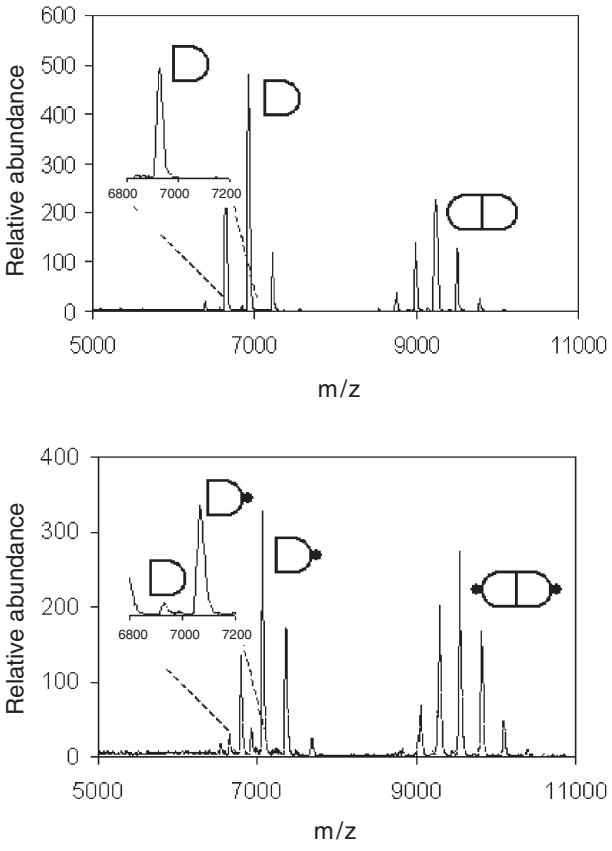

Figure 3. Nanoflow electrospray ionization mass spectra in positive ion mode of native folded Fd-GltS and the complex between Fd-GltS and Fd sprayed from 50 mM ammonium acetate, pH 6.8. Top: The mass spectrum of 1 µM Fd-GltS reveals the monomeric protein at m/z around 7000 (mean charge state +24) and dimeric protein at m/z around 9000 (mean charge state +36). Bottom: The mass spectrum of 1 µM Fd-GltS mixed with 1 µM Fd reveals the equimolar complex between the proteins in both their monomeric form at m/z around 7000 (mean charge state +25) and dimeric form at m/z around 9500 (mean charge state +37). The insets show the zoomed-in part of m/z 6800–7200 and display the relative ion abundance of GltS [M+24H]+ and Fd:Fd-GltS [M+25H]+. The most abundant ion peak of the heterodimeric complex between Fd and Fd-GltS has one charge more than the most abundant peak of Fd-GltS.

For Fd-GltS to produce L-glutamate from L-glutamine and 2-oxoglutarate, reducing equivalents originating from reduced Fd are necessary. Synchrotron radiation X-ray scattering data have shown that Fd-GltS forms an equimolar complex with Fd [4]. The Fd:Fd-GltS complex was also studied by electrospray ionization mass spectrometry, confirming that the two proteins form an equimolar complex (fig. 3). Even when we added a threefold molar excess of Fd to Fd-GltS, we only observed a 1:1 complex with a molecular mass of 176,698 Da, which is in close agreement with the expected mass of a 1:1 complex (176,735 Da including the FMN, [3Fe-4S] and [2Fe-2S] noncovalently bound cofactors). The Fd:Fd-GltS assembly appeared to interact very tightly as the mass spectrometric data of a 1 µM equimolar mixture of

the two proteins revealed nearly complete complex formation (> 90%).

Glutaminase reaction of glutamate synthase

The glutaminase site in the amidotransferase domain catalyzes the hydrolysis of L-glutamine into the first molecule of L-glutamate and ammonia. Ammonia is then transferred to the second catalytic center, where it is added onto 2-oxoglutarate (fig. 1). The fold of the Ntn-type amidotransferases is the signature of the structural superfamily of Ntn hydrolases that appear to be evolutionary related, but have diverged beyond any recognizable primary structure similarity [37]. The substrate binding pocket, the oxyanion hole, the proton donor and the catalytic nucle-

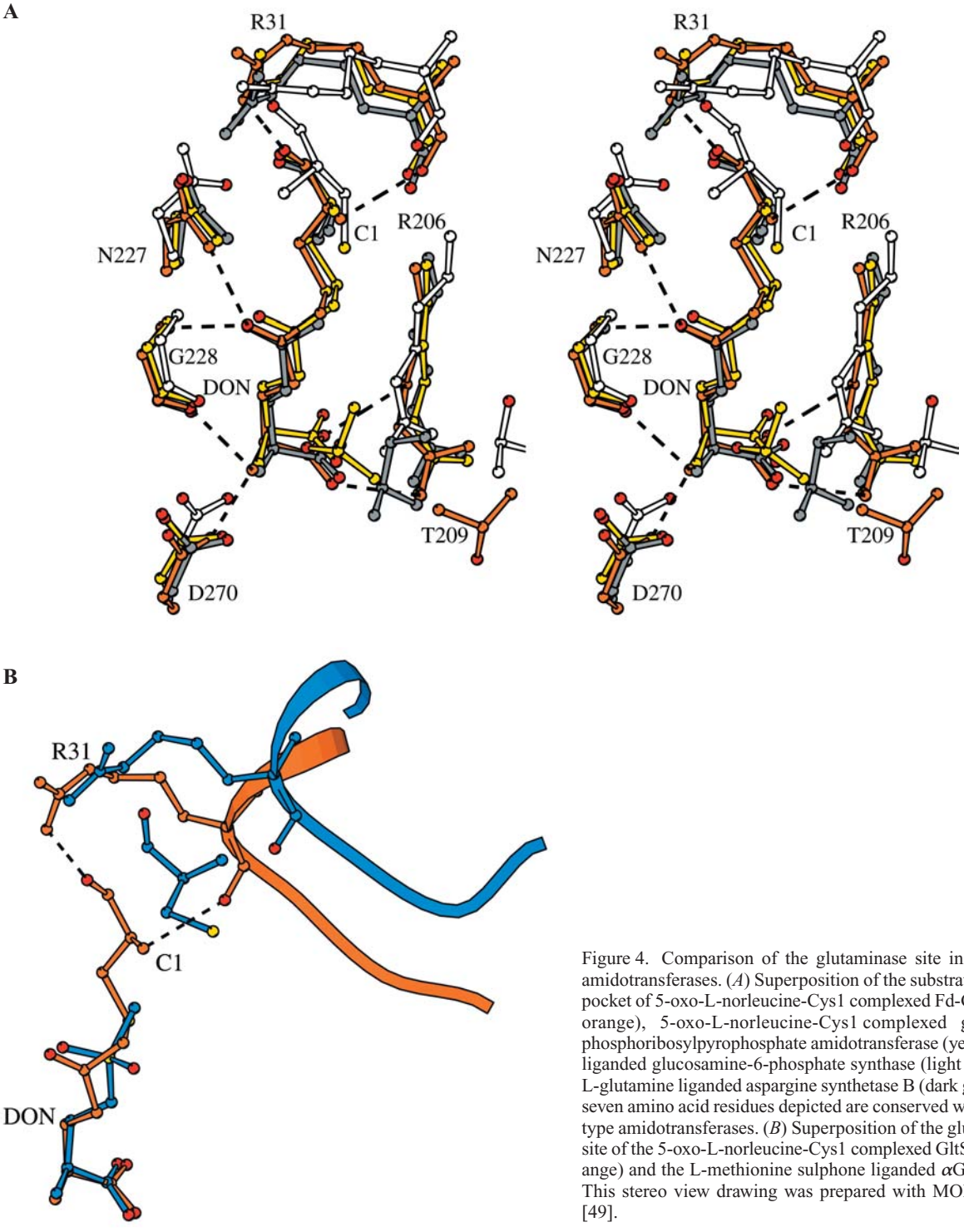

Figure 4. Comparison of the glutaminase site in Ntn-type amidotransferases. (*A*) Superposition of the substrate binding pocket of 5-oxo-L-norleucine-Cys1 complexed Fd-GltS (dark orange), 5-oxo-L-norleucine-Cys1 complexed glutamine phosphoribosylpyrophosphate amidotransferase (yellow), unliganded glucosamine-6-phosphate synthase (light grey) and L-glutamine liganded aspargine synthetase B (dark grey). The seven amino acid residues depicted are conserved within Ntn-type amidotransferases. (*B*) Superposition of the glutaminase site of the 5-oxo-L-norleucine-Cys1 complexed GltS (dark orange) and the L-methionine sulphone liganded αGlts (blue). This stereo view drawing was prepared with MOLSCRIPT [49].

ophile occupy topological equivalent sites in all members of this superfamily. The mechanism of action of L-glutamine hydrolysis in Ntn-type amidotransferases, as discussed below, appears to be similar to that of other Ntn hydrolases even though the nucleophile varies: cysteine in amidotransferases, serine in penicillin acylase and threonine in 20S proteasome and aspartylglucosaminidase. The free N-terminus is thought to be essential for activation of the active site nucleophile (Cys in amidotransferases) and protonation of the leaving group (ammonia in amidotransferases) in the hydrolytic reaction. Moreover, the free N-terminal amino group should participate in deprotonation of the water molecule required to hydrolyze the glutamyl-thioester intermediate [19].

The four members of the Ntn amidotransferase family, GltS [2–4], asparagine synthetase B [25], glutamine phosphoribosylpyrophosphate amidotransferase [23, 38–41] and glucosamine 6-phosphate synthase [24, 42] have been thoroughly characterized, and for all enzymes one or more X-ray structures are known in the free state and/or in complex with substrate (analogues), product or inhibitors. The substrate binding pockets of the four Ntn amidotransferases are remarkably well conserved (fig. 4A). 5-Oxo-L-norleucine in GltS and glutamine phosphoribosylpyrophosphate amidotransferase [39] and L-glutamine in the Cys1 Ala mutant of asparagine synthetase B [25] bind in equivalent positions. L-glutamine is specifically recognized by the glutaminase binding pocket forming an extensive hydrogen bond network with the invariant residues lining the catalytic centre: Cys1, Arg31, Arg206, Thr209, Asn227, Gly228 and Asp270 (numbering according to Fd-GltS) (fig. 4A). The substrate is oriented such that the amide group points with its carbonyl oxygen towards the oxyanion hole (Asn227 and Gly228), its carbon atom is in correct juxtaposition to the nucleophilic sulfur atom of Cys1 and the amide leaving group is within reach of the amino terminus, which acts as the proton donor. The initial binding of the L-glutamine substrate is thought to be followed by closure of the glutamine lid loop (residues 206–214, also known as Q-loop), which protects L-glutamine from bulk solvent. The substrate lid loop in GltS appears to be in the open conformation [2, 3]. Within this loop, only the position of Thr209 is not conserved in GltS with respect to its three homologues in which the glutamine lid loop is (partially) closed (fig. 4A). GltS has been crystallized in both the catalytically active (all structures of Fd-Glts; table 1) and inactive conformations (structure of α-GltS in complex with L-methionine sulphone; table 1) (fig. 4B). By comparing these structures, it appears that the binding of the substrate analogue L-methionine sulphone shifts the position of Cys1 and loop 29–34 out of the substrate-binding pocket so that the enzyme becomes catalytically incompetent [4].

The reaction mechanism by which L-glutamine is hydrolyzed to glutamate and ammonia is thought to occur via nucleophilic attack on the substrate carbonyl atom by the Cys1 thiolate anion (fig. 4A). This initial nucleophilic attack leads to the formation of a covalently bound glutamyl thioester intermediate, which is mimicked by the 5-oxo-L-norleucine-Cys1 adduct in some of the GltS and glutamine phosphoribosylpyrophosphate amidotransferase structures. Indeed, the position of 5-oxo-L-norleucine in the substrate binding pocket is consistent with the proposed mechanism of glutamine hydrolysis [4, 23]. The final product L-glutamate has been cocrystallized with the isolated amidotransferase domain of glucosamine 6-phosphate synthase [42], which is, however, not catalytically competent. However, the position and hydrogen bond interactions of L-glutamate appear to be conserved with respect to the position and hydrogen bond pattern of L-glutamine. The intermediate ammonia product must be kept within the enzyme and gated through an intramolecular tunnel to the synthase site where it is added to an acceptor substrate which differs for each of the amidotransferases: 2-oxoglutarate for GltS (fig. 1), fructose 6-phosphate for glucosamine 6-phosphate synthase, aspartate for asparagine synthetase B and 5-phosphoribosyl-(α)1-pyrophosphate for glutamine phosphoribosylpyrophosphate amidotransferase.

Synthase reaction of glutamate synthase

In the FMN binding domain of GltS, ammonia, originating from the glutaminase site, is added onto 2-oxoglutarate to form the 2-iminoglutarate reaction intermediate. This intermediate product is then reduced by the FMN cofactor to yield the second molecule of L-glutamate (fig. 1). The X-ray models of the FMN binding domains of NADPH-GltS and Fd-GltS are highly similar [2, 3]. Catalysis in the synthase site is formally initiated by the binding of 2-oxoglutarate. The 2.0-Å-resolution X-ray structure of GltS in complex with 2-oxoglutarate has shown unambiguously the positions of all the substrate atoms (fig. 5A). We have demonstrated before that the carbonyl oxygen of 2-oxoxglutarate is stabilized by Lys972 and that the substrate is ideally positioned to receive the ammonia molecule from the intramolecular tunnel [4]. Furthermore, the observed position of 2-oxoglutarate does not allow its reduction by the reduced FMN cofactor, since the distance between C2 of 2-oxoglutarate and N5 of FMN is longer than 4.0 Å and the 2-oxoglutarate C1-C2(O)-C3 plane is not parallel with the FMN isoalloxazine ring.

Insights in catalysis of reductive synthesis of L-glutamate at the FMN binding domain of GltS could be obtained in comparison with the well-characterized flavocytochrome b_2. Flavocytochrome b_2 catalyzes the oxidation of L-lactate to pyruvate with the subsequent transfer of electrons to cytochrome *c*. Thus, the stereochemistry of the GltS-

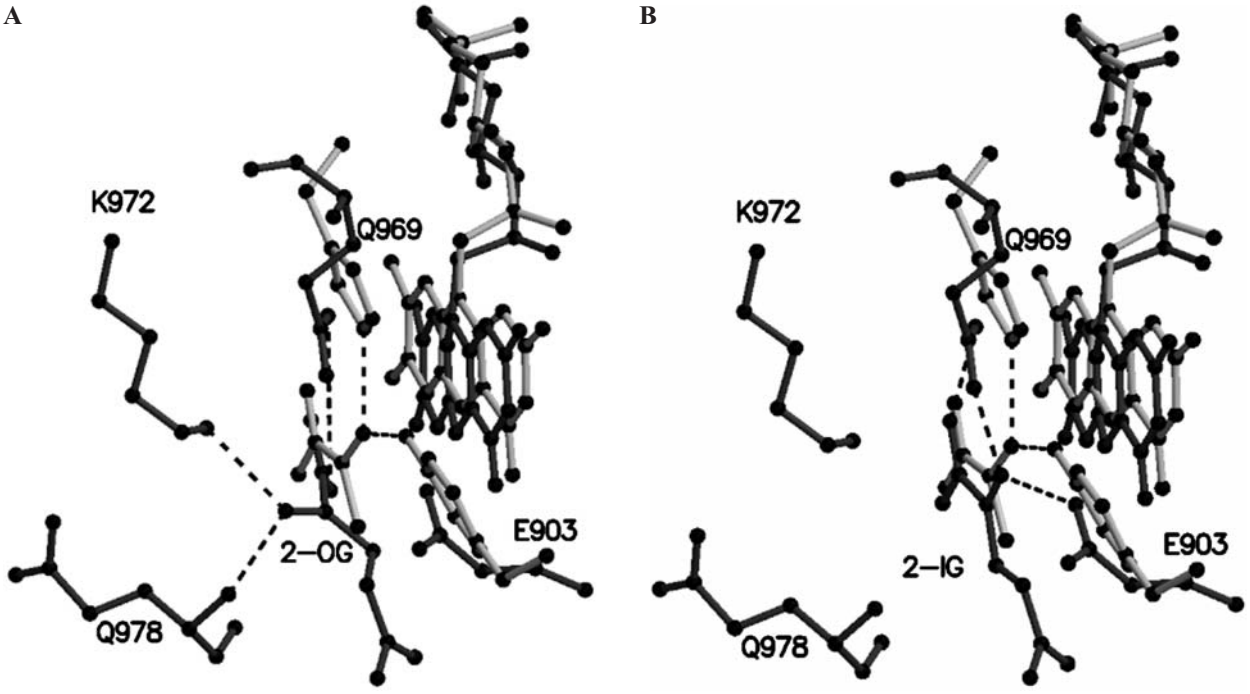

Figure 5. Synthase active site in the FMN binding domain of GltS. (*A*) Superposition of 2-oxoglutarate-liganded Fd-GltS and pyruvate-liganded flavocytochrome b_2. The carbonyl oxygen of 2-oxoglutarate is hydrogen bonded to Lys972 and Gln978, whereas the carbonyl oxygen of pyruvate is hydrogen bonded to Tyr254 and His373. (*B*) Superposition of the modeled 2-iminoglutarate-liganded Fd-GltS and of pyruvate-liganded flavocytochrome b_2. The imino group of 2-iminoglutarate now potentially interacts with Glu903 and Gln969. The latter two residues are spatially equivalent to Tyr254 and His373 in flavocytochrome b_2. This drawing was prepared with MOLSCRIPT [49] and Raster3D [48].

catalyzed reaction is the same as that of flavocytochrome b_2. The enzyme is a homooctamer with a subunit molecular mass of 57.5 kDa containing two noncovalently bound cofactors, FMN and heme, per subunit [43]. Its three-dimensional structure in complex with the reaction product pyruvate has been determined [27]. Pyruvate is bound parallel to the FMN isoalloxazine ring, and the shortest distance between cofactor and product (3.5 Å) involves the flavin N5 atom and the pyruvate carbonyl C2 atom. This position of pyruvate fulfills all requirements for enzyme catalysis. Superposition of the FMN binding domains of GltS and flavocytochrome b_2 clearly reveals the differences between binding of their respective ligands. We have argued that the addition of ammonia to 2-oxoglutarate initiates a rotation of the 2-iminoglutarate product such that this intermediate is properly positioned for reduction by reduced FMN. Thus, the C1-C2(N)-C3 plane is likely to be planar with the FMN isoalloxazine ring, and the distance between C2 2-iminoglutarate and N5 FMN should be about 3.5 Å [4], a conformation similar to that of pyruvate in flavocytochrome b_2. Superposition of a modeled 2-iminoglutarate in the active site of GltS and the X-ray model of pyruvate-liganded flavocytochrome b_2 indicates the homology between the two enzyme active sites (fig. 5B). Mathews and co-workers have postulated that the hydroxyl moiety of L-lactate is hydrogen bonded to His373 and Tyr254, as is the carbonyl oxygen in the pyruvate product [27]. The residues equivalent to Tyr254 and His373 of flavocytochrome b_2 are Glu903 and Gln969 in GltS, respectively, with their side chains pointing in the active site cavity. Indeed, the imine nitrogen of the modeled 2-iminoglutarate may form a hydrogen bond interaction with the side chains of Glu903 and Gln969.

Thus, GltS catalyzes ammonia addition to 2-oxoglutarate and reduction of 2-iminoglutarate in one active site. The charged residues Lys972 and Glu903 appear to be crucial for this dual functionality as Lys972 anchors the carbonyl oxygen of 2-oxoglutarate, fixing the substrate in an orientation that is suited for ammonia addition, but not for reduction by FMN. Lys972 is likely to play a prominent role in catalysis through polarization of the C2 atom, making this atom more prone to nucleophilic attack by ammonia. After 2-iminoglutarate formation, the negative charge of the side chain of Glu903 fixes the intermediate in the proper orientation for reduction by FMN, allowing formation of the second molecule of L-glutamate.

Ammonia tunnel

The X-ray structures of GltS reveal that the glutaminase site and the synthase site are separated by more than 30 Å distance. An internal ammonia tunnel connects the two ac-

tive sites (fig. 2). The tunnel entrance is located close to the amidotransferase active site, at the interface among three domains, namely the amidotransferase domain, the central domain and the C-terminal domain. In different GltS structures, there are no detectable differences in the geometry of the tunnel itself, nor of residues restricting it at either glutaminase or synthase sites. The tunnel points into the FMN binding domain and mainly consists of residues from the FMN binding domain. A major part of one wall of the tunnel is formed by residues 1003–1013, which belong to loop 4 (residues 968–1013) of the FMN-binding $(\beta/\alpha)_8$ barrel [2, 3].

Comparison of the GltS ammonia tunnel with the tunnels in glucosamine 6-phosphate synthase, asparagine synthetase B and glutamine phosphoribosylpyrophosphate amidotransferase reveals marked differences among the four enzymes as also recently pointed out by Raushel and co-workers [44]. The 32-Å-long GltS tunnel consists mainly of backbone atoms of hydrophilic residues, but it also involves the side chains of Glu903, Ser947 and

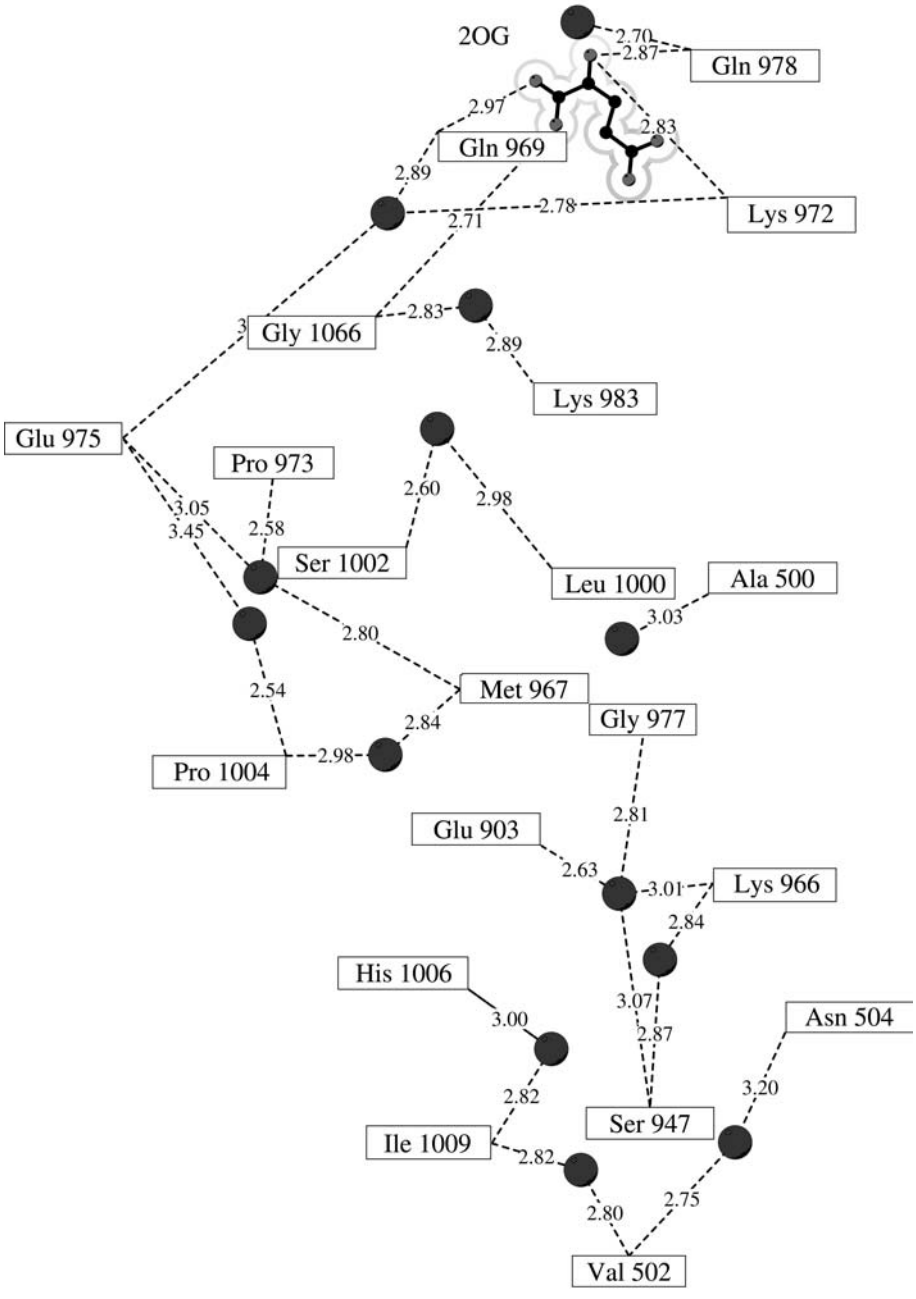

Figure 6. Cartoon of hydrogen bond interactions between ordered water molecules within the GltS ammonia tunnel and the residues lining the tunnel. The 2-oxoglutarate substrate is depicted as ball-and-stick and the water molecules as spheres.

Lys966 [2, 3]. We found several ordered water molecules in the tunnel interacting with residues forming the tunnel via an extensive hydrogen bond network (fig. 6). The water molecules completely fill up the tunnel space, and it seems likely that their positions change upon ammonia transfer during catalysis.

The 20-Å-long ammonia tunnel of glutamine phosphoribosylpyrophosphate amidotransferase is lined with nonpolar residues and consists of a string of small cavities between the active sites, suggesting that conformational breathing of the tunnel is necessary for ammonia channeling. By solving the active and inactive enzyme X-ray structure, Smith and co-workers have demonstrated that the tunnel is formed only transiently during catalysis [23, 40]. When the enzyme is crystallized in the presence of 6-diazo-5-oxo-L-norleucine and a carbocyclic analogue of phosphoribosylpyrophosphate, creating a state which mimics the enzyme just after ammonia release and with substrate bound in the synthase site, the C-terminal helix becomes extensively kinked and the flexible loop becomes ordered forming a molecular tunnel [23]. Like glutamine phosphoribosylpyrophosphate amidotransferase, the ammonia tunnel of glucosamine 6-phosphate synthase is rather hydrophobic and has a length of about 20 Å [24]. In the reported X-ray structure of the holoenzyme the tunnel is accessible for bulk solvent; however, it is speculated that the glutamine lid loop, which covers the active site when product L-glutamate and substrate analog L-glutamate-γ-hydroxamate are bound to the isolated amidotransferase domain [42], closes and isolates the tunnel from solvent upon L-glutamine substrate binding. The length of the molecular tunnel in asparagine synthetase B is also about 20 Å and is formed primarily by backbone atoms and hydrophobic or nonpolar residues. However, the side chain of a glutamate residue is identified at the end of the tunnel near the AMP moiety [25]. The X-ray structure of this enzyme in the presence of L-glutamine and adenosyl monophosphate revealed, as in GltS, several ordered water molecules within the ammonia tunnel.

The observed differences in the molecular structures of the tunnels are not surprising as most of the tunnel is formed in all cases by the synthase domains of the enzymes, which are not related to each other. In GltS, the synthase domain is the FMN binding domain with an $(\alpha/\beta)_8$ topology. The isomerase domain of glucosamine 6-phosphate synthase has a canonical nucleotide-binding fold. The C-terminal domain of asparagine synthetase B is characterized by a five-stranded parallel β sheet flanked on either side by α helices. Finally, the phosphoribosyl transferase domain of glutamine phosphoribosylpyrophosphate amidotransferase consists of a parallel β sheet enclosed by α helices. On the other hand, even in synthase domains with equivalent topologies, ammonia transfer can occur via different molecular mechanisms. For instance, imidazole glycerol phosphate synthase is a triad-type amidotransferase which catalyzes the formation of the imidazole ring in histidine biosynthesis. As in GltS, the synthase domain, harbored in the HisF subunit, exhibits a classical $(\beta/\alpha)_8$ domain topology. However, at variance with GltS, the active site is on the barrel side far from the amidotransferase site, so that the tunnel of imidazole glycerol phosphate synthase runs across the barrel interior [45, 46]. This differs significantly from the tunnel in GltS that runs under loop 4 extending from the C-terminal part of the barrel, where the synthase active site is located.

Enzyme self-regulation

GltS functions through hydrolysis of L-glutamine in the glutaminase site into L-glutamate and ammonia. Ammonia is then transferred through the intramolecular tunnel to the synthase site where it is added to 2-oxoglutarate. The resulting 2-iminoglutarate is reduced by the reduced FMN cofactor, producing the second molecule of L-glutamate (fig. 1). The FMN cofactor in Fd-GltS receives its electrons, via the [3Fe-4S] cluster, from two molecules of reduced Fd. How is the glutaminase activity in Fd-GltS regulated such that L-glutamine is only hydrolyzed when the acceptor substrate 2-oxoglutarate and the reduced electron donating protein Fd are present?

It was proposed earlier that GltS regulates its activity by using a unique mechanism of self-regulation in which loop 4 (residues 968–1013) of the FMN $(\beta/\alpha)_8$ barrel plays an important role [2, 4]. The N-terminal region of loop 4 is in the vicinity of the loop carrying the [3Fe-4S] cluster and of the Fd-binding loop (residues 907–933). Loop 4 is also involved in binding of 2-oxoglutarate through residues Arg992, Lys972 and Gln969, whereas at the C-terminus loop 4 interacts with the catalytic residue Cys1. Figure 7 presents a model of the mechanism of action of Fd-GltS. It is proposed that upon binding of 2-oxoglutarate and of reduced Fd in Fd-GltS, loop 4 shifts from an inactive conformation to the active state in which its C-terminal residue Glu1013 forms a hydrogen bond with Cys1. This interaction activates the glutaminase site such that L-glutamine can bind in the active site cavity. Upon binding of L-glutamine, loop 206–214 is likely to close to prevent solvent molecules from entering the substrate-binding pocket. Now, L-glutamine is hydrolyzed, forming L-glutamate and ammonia. The closed substrate binding pocket shields ammonia from solvent, and therefore ammonia may reach the tunnel without being protonated. Ammonia is transferred from the glutaminase site to the synthase site in a diffusion-controlled manner, after which it is added onto 2-oxoglutarate, producing the 2-iminoglutarate intermediate. The latter rotates such that it becomes properly positioned to be reduced by the reduced FMN prosthetic group (fig. 5B). In the final step 2-

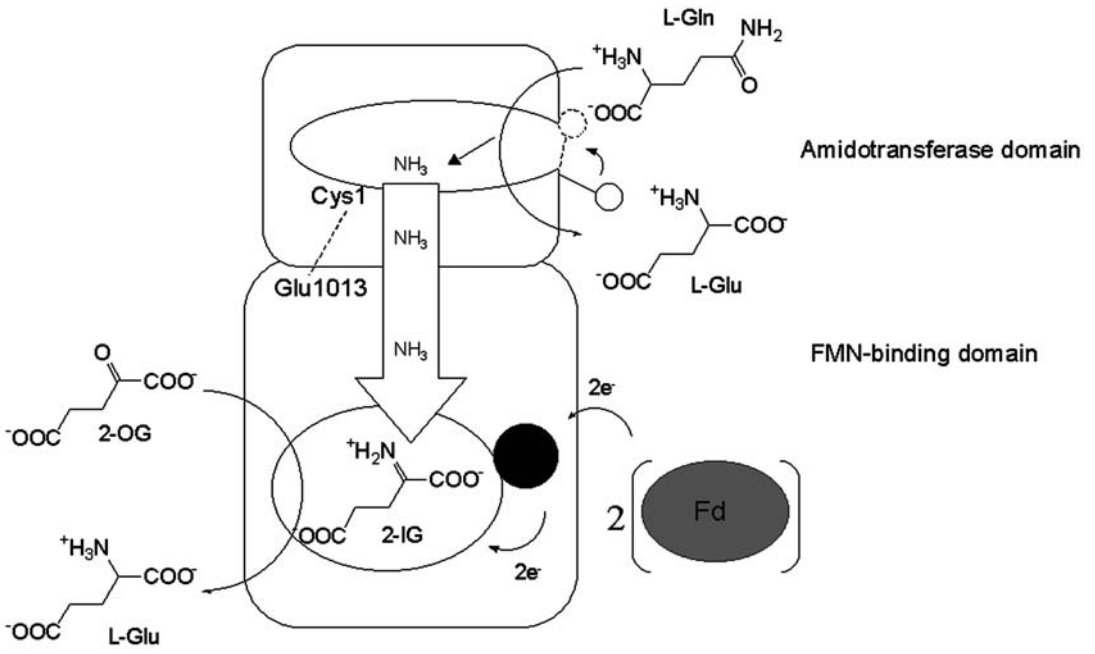

Figure 7. Cartoon predicting the mechanism of action and self-regulation of GltS [1, 4, 6]. Catalysis is initiated by the binding of 2-Oxoglutarate and reduced Fd to the FMN binding domain, followed by reduction of the FMN cofactor. Loop 4 is now subject to (small) conformational changes, which eventually lead to hydrogen bond interaction between Glu1013 (C-terminus of loop 4) and the catalytic Cys1 residue. The glutaminase site in the amidotransferase domain is in the proper conformation for L-glutamine binding. The glutamine lid loop (residues 206–214) closes to protect the substrate binding pocket from bulk solvent, and L-glutamine is hydrolyzed, forming the first molecule of L-glutamate and ammonia. L-Glutamate is released, and ammonia is transferred through the intramolecular tunnel in a diffusion-dependent manner and added onto the C2 atom of 2-oxoglutarate. The formed 2-iminoglutarate intermediate is positioned such that reduced FMN can reduce the intermediate to the second molecule of L-glutamate, after which the cycle can start over again.

iminoglutarate is reduced by FMN and the second molecule of L-glutamate is released. As discussed previously, Met475 may also contribute to the complex regulation of GltS activity [2]. This residue is in contact with both the [3Fe-4S] cluster and the FMN cofactor, and it may sense the cofactor's redox state, transmitting such a signal to the amidotransferase domain and the ammonia tunnel.

In conclusion, enzyme self-regulation and ammonia channeling are common solutions found in all amidotransferases for efficient catalysis without wasteful consumption of substrates and intermediates and to transfer the amide nitrogen from L-glutamine to the acceptor substrate. However, while amidotransferase domains are conserved and fall in the two well characterized triad and Ntn-type classes of enzymes, both the properties of ammonia tunnels and the mechanisms of control and coordination of catalysis at the glutaminase and synthase sites differ among the known glutamine-dependent amidotransferases. Furthermore, the acceptor domains are unrelated to each other. These observations indicate that amidotransferases have evolved independently from each other through recruitment of preexisting protein functions. In the case of amidotransferases, it appears to have been an easier task for the enzymes to recruit and optimize separately two enzymatic functions, and design a means to transfer the reaction intermediate, than to accommodate the ancestral separate enzymatic functions in a single functional active site. In light of the properties of ammonia, for which, at variance with, for example, acetyl groups in lipoate-dependent enzymes or CO_2 in biotin-dependent enzymes there is no carrier, intramolecular tunnels seem to have been the successful common solution found for its transfer in all these enzymes.

Acknowledgements. R. H. H. van den H. was supported by a Marie Curie Fellowship (HPMF-CT-2000–00786) from the European Community. This work was supported by grants from the Ministero della Università e Ricerca Scientifica e Tecnologica (Progetti FIRB, PRIN01 and Legge 449/97). We thank A. Coda and F. J. Florencio for helpful discussions and support during the glutamate synthase project.

1 Vanoni M. A. and Curti B. (1999) Glutamate synthase: a complex iron-sulfur flavoprotein. Cell. Mol. Life Sci. **55**: 617–638
2 Binda C., Bossi R. T., Wakatsuki S., Arzt S., Coda A., Curti B. et al. (2000) Cross-talk and ammonia channeling between active centers in the unexpected domain rearrangement of glutamate synthase. Structure (Camb.) **8**: 1299–1308
3 van den Heuvel R. H. H., Ferrari D., Bossi R. T., Ravasio S., Curti B., Vanoni M. A. et al. (2002) Structural studies on the synchronization of catalytic centers in glutamate synthase. J. Biol. Chem. **277**: 24579–24583
4 van den Heuvel R. H. H., Svergun D. I., Petoukhov M. V., Coda A., Curti B., Ravasio S. et al. (2003) The active conformation of

glutamate synthase and its binding to ferredoxin. J. Mol. Biol. **330**: 113–128
5 Ravasio S., Dossena L., Martin-Figueroa E., Florencio F. J., Mattevi A., Morandi P. et al. (2002) Properties of the recombinant ferredoxin-dependent glutamate synthase of *Synechocystis* sp. PCC 6803. Comparison with the *Azospirillum brasilense* NADPH-dependent enzyme and its isolated α subunit. *Biochemistry* **41**: 8120–8133
6 Vanoni M. A., Nuzzi L., Rescigno M., Zanetti G. and Curti B. (1991) The kinetic mechanism of the reactions catalyzed by the glutamate synthase from *Azospirillum brasilense*. Eur. J. Biochem. **202**: 181–189
7 Tempest D. W., Meers J. L. and Brown C. M. (1970) Synthesis of glutamate in *Aerobacter aerogenes* by a hitherto unknown route. Biochem. J. **117**: 405–407
8 Lea P. J., Robinson S. A. and Stewart G. R. (1990) The enzymology and metabolism of glutamine, glutamate and asparagine. In: The Biochemistry of Plants, vol. 16, pp. 121–159, Miflin B. J. and Lea P. J. (eds), Academic Press, New York
9 Temple S. J., Vance C. P. and Gantt J. S. (1998) Glutamate synthase and nitrogen assimilation. Trends Plant Sci. **3**: 51–56
10 Lea P. J. and Ireland R. J. (1999) Nitrogen metabolism in higher plants. In: Plant Amino Acids: Biochemistry and Biotechnology, pp. 1–47, Singh B. K. (ed.), Marcel Dekker, New York
11 Reitzer L. J. (1996) Ammonia assimilation and the biosynthesis of glutamine, glutamate, aspartate, asparagine, L-alanine and D-alanine. In: *Escherichia coli* and *Salmonella:* Cellular and Molecular Biology, vol. 1, pp. 391–407, Neidhart F. C. (ed.), ASM Press, Washington, DC
12 Hirasawa M., Hurley J. K., Salamon Z., Tollin G. and Knaff, D. B. (1996) Oxidation-reduction and transient kinetic studies of spinach ferredoxin-dependent glutamate synthase. Arch. Biochim. Biophys. **330**: 209–215
13 Navarro F., Martin-Figueroa E., Candau P. and Florencio F. J. (2000) Ferredoxin-dependent iron-sulfur flavoprotein glutamate synthase (GlsF) from the cyanobacterium *Synechocystis* sp. PCC 6803: expression and assembly in *Escherichia coli*. Arch. Biochem. Biophys. **379**: 267–276
14 Vanoni M. A., Fischer F., Ravasio S., Verzotti E., Edmondson D. E., Hagen W. H. et al. (1998) The recombinant α subunit of glutamate synthase: spectroscopic and catalytic properties. Biochemistry **37**: 1828–1838
15 Vanoni M. A., Verzotti E., Zanetti G. and Curti B. (1996) Properties of the recombinant β subunit of glutamate synthase. Eur. J. Biochem. **236**: 937–946
16 Buchanan J. M. (1973) The amidotransferases. Adv. Enzymol. **39**: 91–183
17 Massière F. and Badet-Denison M.-A. (1998) The mechanism of glutamine amidotransferases. Cell. Mol. Life Sci. **54**: 205–222
18 Zalkin H. (1993) The amidotransferases. Adv. Enzymol. Relat. Areas Mol. Biol. **66**: 203–309
19 Zalkin H. and Smith J. L. (1998) Enzymes utilizing glutamine as an amide donor. Adv. Enzymol. Relat. Areas Mol. Biol. **72**: 87–144
20 Curnow A. W., Hong K., Yuan R., Kim S., Martins O., Winkler W. et al. (1997) Glu-tRNA^{Gln} amidotransferase: a novel heterodimeric enzyme required for correct decoding of glutamine codons during translation. Proc. Natl. Acad. Sci. USA **94**: 11819–11826.
21 Kobayashi M., Fujiwara Y., Goda M., Komeda H. and Shimizu S. (1997) Identification of active sites in amidases: evolutionary relationship between amide bond- and peptide bond-cleaving enzymes. Proc. Natl. Acad. Sci. USA **94**: 11986–11991
22 Nesbo C. L., L'Haridon S., Stetter K. O. and Doolittle W. F. (2001) Phylogenetic analyses of two 'archaeal' genes in *Thermotoga maritima* reveal multiple transfers between archaea and bacteria. Mol. Biol. Evol. **18**: 362–375
23 Krahn J. M., Kim J. H., Burns M. R., Parry R. J., Zalkin H. and Smith J. L. (1997) Coupled formation of an amidotransferase interdomain ammonia channel and a phosphoribosyltransferase active site. Biochemistry **36**: 11061–11068
24 Teplyakov A., Obmolova G., Badet B. and Badet-Denisot M. A. (2001) Channeling of ammonia in glucosamine 6-phosphate synthase. J. Mol. Biol. **313**: 1093–1102
25 Larsen T. M., Boehlein S. K., Schuster S. M., Richards N. G., Thoden J. B., Holden H. M. et al. (1999) Three-dimensional structure of *Escherichia coli* asparagine synthetase B: a short journey from substrate to product. Biochemistry **38**: 16146–16157
26 Holm L. and Sander C. (1993) Protein structure comparison by alignment of distance matrices. J. Mol. Biol. **233**: 123–138
27 Xia Z. X. and Mathews F. S. (1990) Molecular structure of flavocytochrome b2 at 2.4 Å resolution. J. Mol. Biol. **212**: 837–863
28 Lindqvist Y. (1989) Refined structure of spinach glycolate oxidase at 2 Å resolution. J. Mol. Biol. **209**: 151–166
29 Rowland P., Nielsen F. S., Jensen K. F. and Larsen S. (1997) The crystal structure of the flavin containing enzyme dihydroorotate dehydrogenase A from *Lactococcus lactis*. Structure (Camb.) **5**: 239–252
30 Lang D., Thoma R., Henn-Sax M., Sterner R. and Wilmanns M. (2000) Structural evidence for evolution of the $(\beta/\alpha)_8$ barrel scaffold by gene duplication and fusion. Science **289**: 1546–1550
31 Hocker B., Beismann-Driemeyer S., Hettwer S., Lustig A. and Sterner R. (2001) Dissection of a $(\beta/\alpha)_8$ barrel enzyme into two-folded halves. Nat. Struct. Biol. **8**: 32–36
32 Pickersgill R., Smith D., Worboys K. and Jenkins J. (1998) Crystal structure of polygalacturonase from *Erwinia carotovora* ssp. *carotovora*. J. Biol. Chem. **273**: 24660–24664
33 Akita M., Suzuki A., Kobayashi T., Ito S. and Yamane T. (2000) The first structure of pectate lyase belonging to polysaccharide lyase family 3. Acta Crystallogr. Sec. D-Biol. Crystallogr. **57**: 1786–1792
34 Petoukhov M. V., Svergun D. I., Kornarev P. V., Ravasio S., van den Heuvel R. H. H., Curti B. and Vanoni M. A. (2003) Quaternary structure of *Azospirillum brasilense* NADPH-dependent glutamate synthase in solution as revealed by synchrotron radiation X-ray scattering. J. Biol. Chem. **278**: 29933–29939
35 Reference removed in proof
36 Stabile H., Curti B. and Vanoni M. A. (2000) Functional properties of recombinant *Azospirillum brasilense* glutamate synthase, a complex iron-sulfur flavoprotein. Eur. J. Biochem. **267**: 2720–2730
37 Brannigan J. A., Dodson G., Duggleby H. J., Moody P. C., Smith J. L., Tomchick D. R. et al. (1995) A protein catalytic framework with an N-terminal nucleophile is capable of self-activation. Nature **378**: 416–419
38 Chen S., Tomchick D. R., Wolle D., Hu P., Smith J. L., Switzer R. L. et al. (1997) Mechanism of the synergistic end-product regulation of *Bacillus subtilis* glutamine phosphoribosylpyrophosphate amidotransferase by nucleotides. Biochemistry **36**: 10718–10726
39 Kim J. H., Krahn J. M., Tomchick D. R., Smith J. L. and Zalkin H. (1996) Structure and function of the glutamine phosphoribosylpyrophosphate amidotransferase glutamine site and communication with the phosphoribosylpyrophosphate site. J. Biol. Chem. **271**, 15549–15557
40 Muchmore C. R. A., Krahn J. M., Kim J. H., Zalkin H. and Smith J. L. (1998) Crystal structure of glutamine phosphoribosylpyrophosphate amidotransferase from *Escherichia coli*. Protein Sci. **7**: 39–51
41 Smith J. L., Zaluzec E. J., Wery J.-P., Niu L., Switzer R., Zalkin H. et al. (1994) Structure of the allosteric regulatory enzyme of purine biosynthesis. Science **264**: 1427–1433
42 Isupov M. N., Obmolova G., Butterworth S., Badet-Denisot M. A., Badet B., Polikarpov I. et al. (1996) Substrate binding is required for assembly of the active conformation of the catalytic site in Ntn amidotransferases: evidence from the 1.8 Å crystal

structure of the glutaminase domain of glucosamine 6-phosphate synthase. Structure (Camb.) **4**: 801–810
43 Jacq C. and Lederer F. (1974) Cytochrome b_2 from bakers' yeast (L-lactate dehydrogenase). A double-headed enzyme. Eur. J. Biochem. **41**: 311–320
44 Raushel F. M., Thoden J. B. and Holden H. M. (2003) Enzymes with molecular tunnels Acc. Chem. Res. **36**: 539–548
45 Chauduri B. N., Lange S. C., Myers R. S., Chittur S. V., Davisson V. J. and Smith J. L. (2001) Crystal structure of imidazole glycerol phosphate synthase: a tunnel through a $(\alpha/\beta)_8$ barrel joins two active sites. Structure (Camb.) **9**: 987–997
46 Douangamath A., Walker M., Beismann-Driemeyer S., Vega-Fernandez M. C., Sterner R. and Wilmanns M. (2002) Structural evidence for ammonia tunneling across the $(\beta/\alpha)8$ barrel of the imidazole glycerol phosphate synthase bienzyme complex. Structure (Camb.) **10**: 185–93
47 Lawrence M. C. and Bourke P. (2000) CONSCRIPT: a program for generating electron density isosurfaces from Fourier syntheses in protein crystallography. J. Appl. Cryst. **33**: 990–991
48 Merritt E. A. and Bacon D. J. (1997) Raster3D: photorealistic molecular graphics. Methods Enzymol. **277**: 505–524
49 Kraulis P. J. (1991) MOLSCRIPT: a program to produce both detailed and schematic plots of protein structures. J. Appl. Crystallogr. **24**: 946–950